

# Effect of grain size on microstructure, properties and surface roughness of reaction bonded SiC ceramics

Michael Aghajanian<sup>\*a</sup>, Craig Emmons<sup>b</sup>, Steve Rummel<sup>c</sup>, Paul Barber<sup>c</sup>, Chris Robb<sup>d</sup>, Doug Hibbard<sup>d</sup>

<sup>a</sup>M Cubed Technologies, 1 Tralee Industrial Park, Newark, DE USA 19711;

<sup>b</sup>M Cubed Technologies, 921 Main Street, Monroe, CT USA 06468;

<sup>c</sup>II-VI Infrared, 375 Saxonburg Blvd, Saxonburg, PA USA 16056;

<sup>d</sup>LightWorks Optical Systems, 36570 Briggs Road, Murrieta, CA USA 92563

## ABSTRACT

Silicon carbide (SiC) based ceramics have received significant study for optical applications due to high specific stiffness, high thermal conductivity, and low coefficient of thermal expansion (CTE). Reaction bonded SiC ceramics, which are composites of SiC and Si, are of particular interest due to large size and complex shape capability. The behavior of these ceramics is very much affected by the grain size of the SiC phase. The present work examines SiC grain sizes ranging from 6 to 50  $\mu\text{m}$ , with the goal of optimizing properties and finishing capability for optical uses. Microstructures are reviewed; physical, mechanical and thermal properties are presented; and post-polishing surface roughness data are provided. In particular, results demonstrate that properties can be tailored by SiC particle size selection, and that measureable enhancement in surface roughness can be achieved by moving to smaller SiC grain size.

**Keywords:** Silicon Carbide, Reaction Bonding, Direct Polishing, Optics

## 1. INTRODUCTION

Reaction bonded silicon carbide (RBSC) composites are two-phase materials consisting of silicon carbide (SiC) and silicon (Si). The materials are produced with the process steps schematically outlined in Figure 1. Specifically, a porous preform of SiC particles and carbon is produced, and then infiltrated with molten Si. During the infiltration process, the Si and carbon react to form SiC. Therefore, the final body consists of three constituents, namely the original SiC particles, reaction formed SiC, and residual Si. The volume of reaction formed SiC is greater than that of the original carbon (e.g., in the case of graphite, the expansion to SiC is 2.3 x). Thus, as shown in Figure 2<sup>1</sup>, the final SiC:Si ratio of a RBSC ceramic can be controlled by the SiC to carbon ratio of the starting preform.

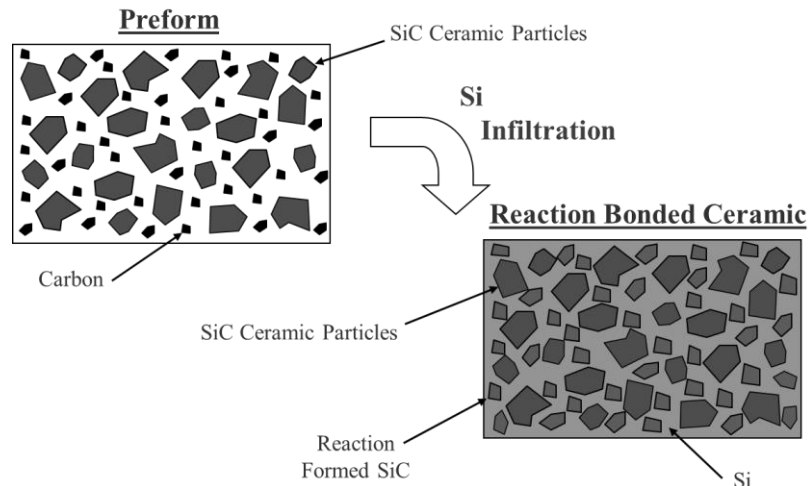


Figure 1. Process Schematic for Reaction Bonded Silicon Carbide

\*aghajanian@mmmt.com; phone 302-454-8600, x304; fax 302-454-8605; mmmmt.com

Michael Aghajanian, MCT; Craig Emmons, MCT; Steve Rummel, II-VI; Paul Barber, II-VI; Chris Robb, LWOS; Doug Hibbard, LWOS; "Effect of grain size on microstructure, properties, and surface roughness of reaction bonded SiC ceramics," Material Technologies and Applications to Optics, Structures, Components, and Sub-Systems; Joseph L. Robichaud, Matthias Krödel, William A. Goodman; Volume 8837, Page 88370J, 2013 Copyright 2013 Society of Photo-Optical Instrumentation Engineers. One print or electronic copy may be made for personal use only. Systematic reproduction and distribution, duplication of any material in this paper for a fee or commercial purposes, or modification of the content of the paper are prohibited.

<http://dx.doi.org/10.1117/12.2024308>

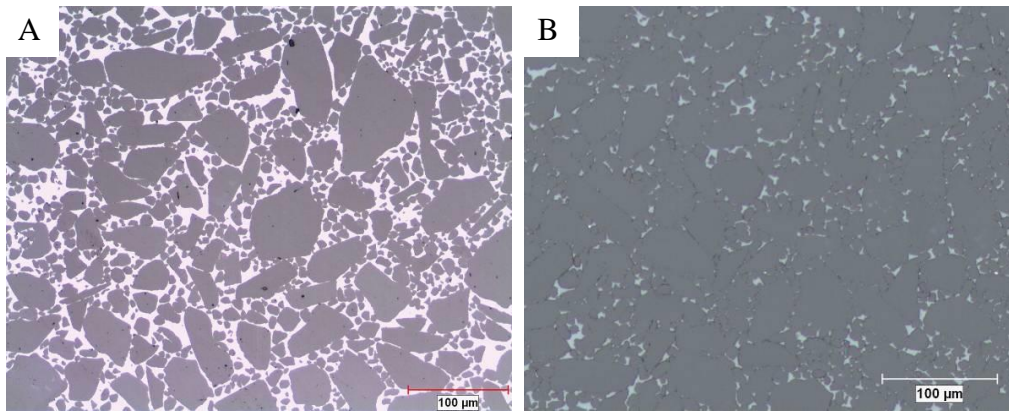


Figure 2. Optical photomicrographs of RBSC ceramics: (A) – SiC to Si ratio of 70:30 formed with low carbon content preform; and, (B) – SiC to Si ratio of 90:10 formed with high carbon content preform

By varying parameters such as particle size, carbon content, SiC:Si ratio, infiltration alloy composition, and preforming method, RBSC ceramics with a wide range of microstructures and properties can be produced<sup>2-4</sup>. In addition, because < 1% process shrinkage occurs (i.e., reaction bonding process fills void space via infiltration rather than shrinkage as with sintering), significant ability to produce large and complex shapes exists<sup>5-6</sup>. Based on these attributes, RBSC ceramics are used in a wide range of applications, including semiconductor capital equipment, furnace components, armor, wear resistant structures, high temperature components, motion control stages/beams, bearings/seals, automotive components, aerospace structures, and corrosion resistant bodies.

In addition to traditional ceramic applications, RBSC ceramics have received interest as optical substrate materials<sup>7-13</sup> due to their combination of properties (high stiffness, low density, high thermal conductivity, low CTE, high heat load capacity, long-term dimensional stability, etc.) and shape making capability. In particular, the complex shape capability of RBSC provides low cost relative to other versions of SiC, and allows thin-walled ribbed geometries to be produced, which yields optical substrates with low areal density, high stiffness, and high natural frequency. Moreover, because RBSC ceramics have pore-free microstructures, they have received interest as directly polishable substrates<sup>8,10</sup>. That is, after the Si infiltration step, a RBSC body consists of interconnected SiC and molten Si that must be then cooled to room temperature, during which time the Si phase solidifies. Because Si expands upon solidification, the resultant microstructure is fully dense. The present work aims to quantify the surface roughness capability (i.e., direct polishability) of RBSC by evaluating a range of materials with systematically controlled grain size, together with assessing the effect of SiC grain size on other critical properties.

The alternative to directly polishing the RBSC ceramic is to apply a polishable cladding to the surface, such as plasma-enhanced, chemical vapor deposited Si (PE-CVD Si)<sup>11</sup> or CVD-SiC<sup>8</sup>. However, issues exist with this approach, including long process lead time, high cost, induced thermal errors with PE-CVD Si due to bi-metallic strip stress associated with different CTEs of the RBSC substrate and Si cladding<sup>10</sup>, and size limitations of PE-CVD and CVD processes (e.g., 1 m maximum for PE-CVD Si<sup>13</sup>).

## 2. EXPERIMENTAL PROCEDURES

SiC particle preforms were produced by casting with three different SiC particle sizes, namely 6, 12 and 50 μm. In the case of the 6 and 12 μm particle sizes, preforms were produced directly with the powders, leading to bodies with mono-sized SiC particles. For the 50 μm particle size, preforms were produced with a blend of 50 and 12 μm powders to yield a particle size distribution that was sufficiently stable for effective casting. In all cases, the preforms contained a low carbon content to yield final microstructures with more-or-less isolated SiC particles within a Si matrix (i.e., limited formation of reaction-formed SiC). After casting, each preform was identically infiltrated with molten Si in a vacuum atmosphere at nominally 1500°C.

After the fabrication step, various mechanical, thermal, and physical properties of the materials were measured using the test methods summarized in Table 1, with the goal of correlating response to grain size. In addition, microstructure was examined optically using a LEICA DM 2500 M microscope and a Clemex JS-2000 digital scanning image analysis system.

Table 1. Summary of test methods used to characterize properties of RBSC composites

Property	Technique	Standard
Density	Immersion	ASTM C 135
Young's Modulus	Ultrasonic Pulse Echo	ASTM E 494
Poisson's Ratio		
Hardness	Knoop (2 kg load)	ASTM C 1326
Flexural Strength	Four Point Bend	ASTM C 1161
Fracture Toughness	Four Point Bend Chevron Notch	ASTM C 1421
Thermal Conductivity	Laser Flash	ASTM E 1461
Coef. of Thermal Expansion	Dilatometry	ASTM E 831

For optical surface roughness characterization, representative samples of each material were similarly prepared by two different fabrication shops. Three consecutive process steps were utilized, namely diamond grinding, diamond lapping, and multiple polishing steps using diamond slurries with successively smaller particle size (down to sub-micron). After polishing, the surface roughness of the samples was measured per ISO Standard 25178 using a white light interferometer. Specifically, the surface roughness data are reported as root mean square (rms) height of the surface.

### 3. RESULTS AND DISCUSSION

Optical photomicrographs of the three material types are provided in Figures 3 and 4. In each case, the dark phase is SiC and the light phase is Si. The dramatic difference in grain size is clearly evident. Also, the desired microstructure of more-or-less isolated SiC particles within a Si matrix is demonstrated. With this feature, as opposed to an interconnected SiC structure as shown in Figure 2B, the effect of the change in particle size on properties and surface roughness will be strongest. Finally, the bi-modal SiC particle size distribution in the 50  $\mu\text{m}$  ceramic (i.e., mixture of 50 and 12  $\mu\text{m}$  particles) is clearly evident. As discussed above, the addition of the smaller particles to the 50  $\mu\text{m}$  formulation was required to allow stable preform casting.

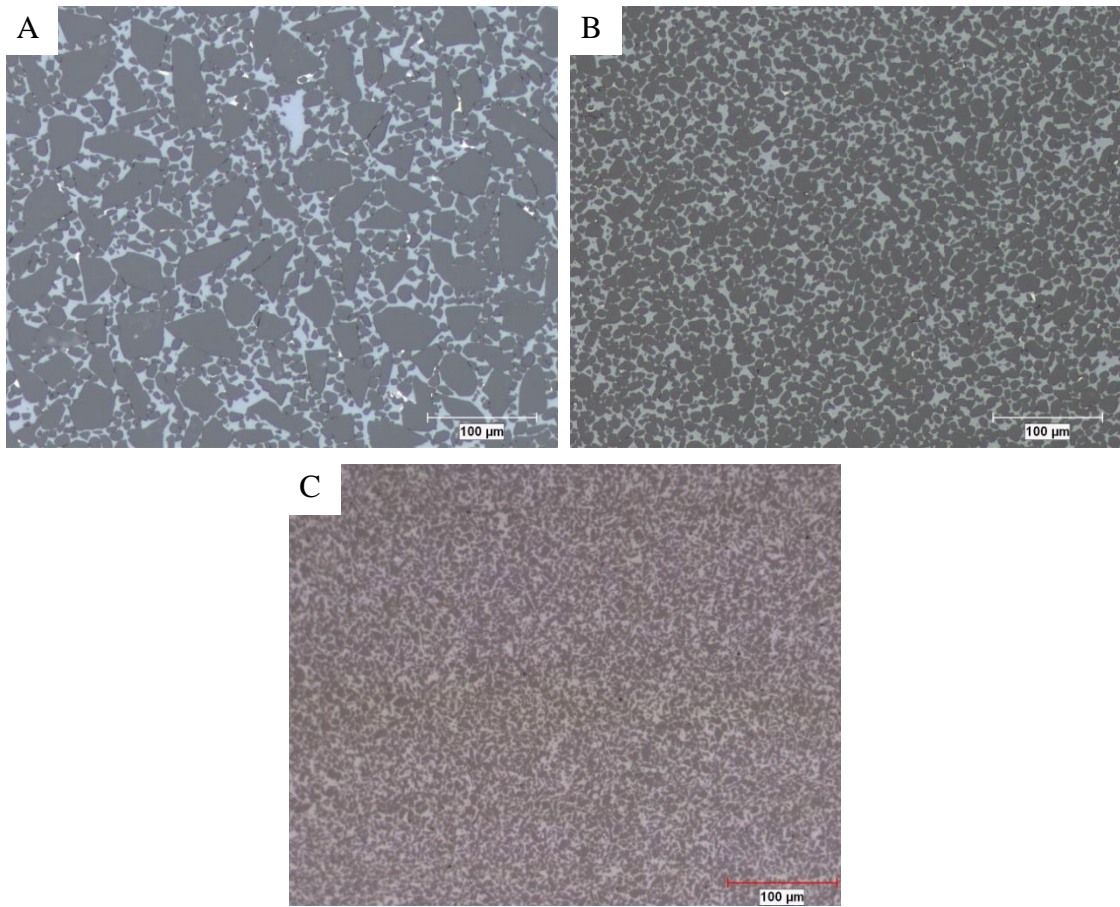


Figure 3. Same magnification optical photomicrographs of (A) 50, (B) 12, and (C) 6 μm particle size RBSC

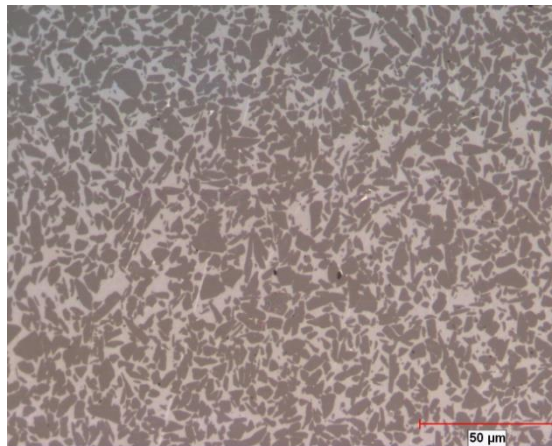


Figure 4. Higher magnification optical photomicrograph of 6 μm particle size RBSC showing isolated SiC particles within Si matrix

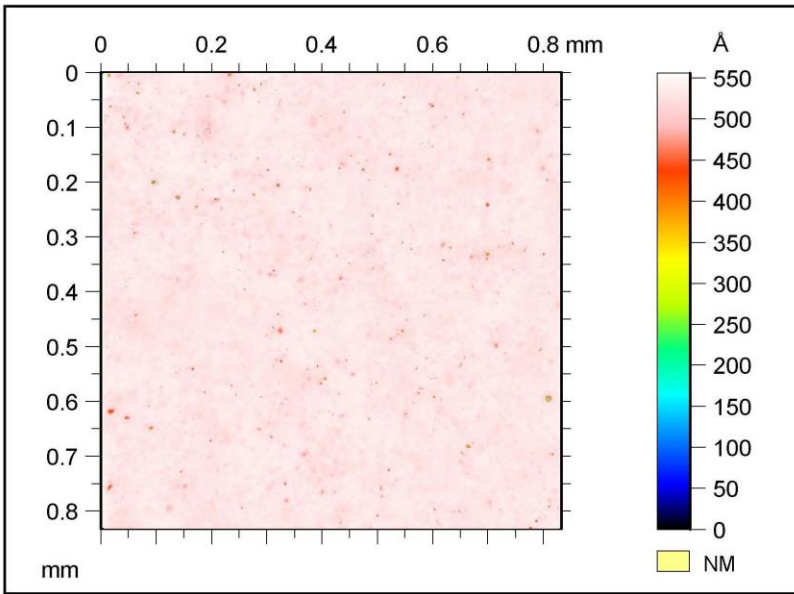
Results of property measurements are provided in Table 2. As anticipated, finer grain size led to lower SiC content (higher Si concentration) due to less particle packing. In addition the bi-modal particle size distribution used in the 50  $\mu\text{m}$  ceramic led to further enhanced SiC particle packing.

Table 2. Effect of SiC grain size on properties of RBSC ceramics

SiC Grain Size ( $\mu\text{m}$ )	RBSC Ceramics		
	6	12	50
SiC Content (vol. %)	66	69	78
Density (g/cc)	2.92	2.95	3.02
Young's Modulus (GPa)	323	344	368
Poisson's Ratio	0.19	0.19	0.19
Hardness ( $\text{kg/mm}^2$ )	1196	1157	1246
Flexural Strength (MPa)	380	351	294
Fracture Toughness ( $\text{MPa}\cdot\text{m}^{1/2}$ )	4	4	4
Thermal Conductivity (W/mK)	137	151	188
Coef. Thermal Exp, 20-100°C (ppm/K)	3.2	3.0	2.9

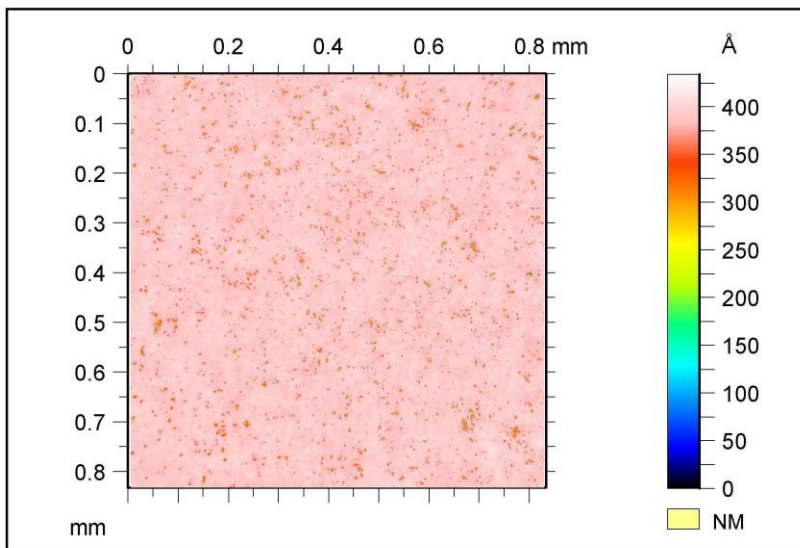
Young's modulus (stiffness) increased with increasing SiC content, as expected, with the values of monolithic SiC and Si being  $450^{14}$  and  $113 \text{ GPa}^{15}$ , respectively. Finer grained polycrystalline ceramics generally have higher hardnesses, other parameters being equal, due to a Hall-Petch-like relationship<sup>16</sup>. Thus, despite lower SiC content, the hardness of the 6  $\mu\text{m}$  ceramic measured as high as that for the 12  $\mu\text{m}$  ceramic. Due to much higher SiC content, the 50  $\mu\text{m}$  ceramic showed the greatest hardness despite its coarser grain size. Consistent with data in the literature<sup>1, 17-18</sup>, a strong relationship between grain size and strength was observed, with nearly a 30% strength increase from the 50 to 6  $\mu\text{m}$  ceramic. The critical flaw size in reaction bonded ceramics has consistently been shown to be related to the grain size, thus leading to the increased strength with smaller particle sizes. In general, coarser grained ceramics tend to have higher values of fracture toughness due to R-curve behavior<sup>19</sup>. In the present study, however, a toughness difference was not identified. Potentially, a test that provides more resolution would be required to identify differences. If required for a given application, achieving increased toughness in RBSC ceramics has been demonstrated with the addition of fiber and/or carbon-nanotube (CNT) reinforcements<sup>9, 20-21</sup>. The thermal property results followed expected trends. First, thermal conductivity decreased as particle size decreases. This trend is well known in particulate-reinforced composites, and is attributed to increased interfaces with smaller grain size, with the interfaces acting as thermal barriers<sup>22-23</sup>. Finally, the trend of increasing CTE with decreasing SiC content followed data in the literature<sup>22</sup>, as the CTE of Si is higher than the CTE of SiC in the 20 to 100°C temperature range.

RBSC ceramics can be directly polished to low roughness due to their fully dense microstructures. However, due to a two-phase microstructure composed of SiC and Si, limitations exist. Schwartz<sup>10</sup> states that it is challenging to reach roughness values below 20  $\text{\AA}$  rms with bare RBSC because of the differing polishing rates of SiC and Si. This is what has driven the need for cladding the RBSC with a more homogeneous SiC or Si layer. For example, Duston<sup>11</sup> presents < 3  $\text{\AA}$  rms roughness for a Si clad (PE-CVD) RBSC mirror and Robichaud<sup>8</sup> presents < 1  $\text{\AA}$  rms roughness for a SiC clad (CVD) RBSC mirror. For the present project, the bare 6, 12 and 50  $\mu\text{m}$  materials were polished in a similar fashion and then compared to yield a relationship between grain size and surface roughness capability. Results of the activity are provided in Figures 5-7.



ISO 25178		
Height Parameters		
<b>Sq</b>	7.98	Å
<b>Ssk</b>	-12	
<b>Sku</b>	409	
<b>Sp</b>	26.6	Å
<b>Sv</b>	529	Å
<b>Sz</b>	556	Å
<b>Sa</b>	4.51	Å

Figure 5. Surface roughness result (6  $\mu\text{m}$  grain size ceramic – 7.98 Å rms (Sq))



ISO 25178		
Height Parameters		
<b>Sq</b>	11.7	Å
<b>Ssk</b>	-8.4	
<b>Sku</b>	122	
<b>Sp</b>	44.8	Å
<b>Sv</b>	389	Å
<b>Sz</b>	434	Å
<b>Sa</b>	5.51	Å

Figure 6. Surface roughness result (12  $\mu\text{m}$  grain size ceramic – 11.7 Å rms (Sq))

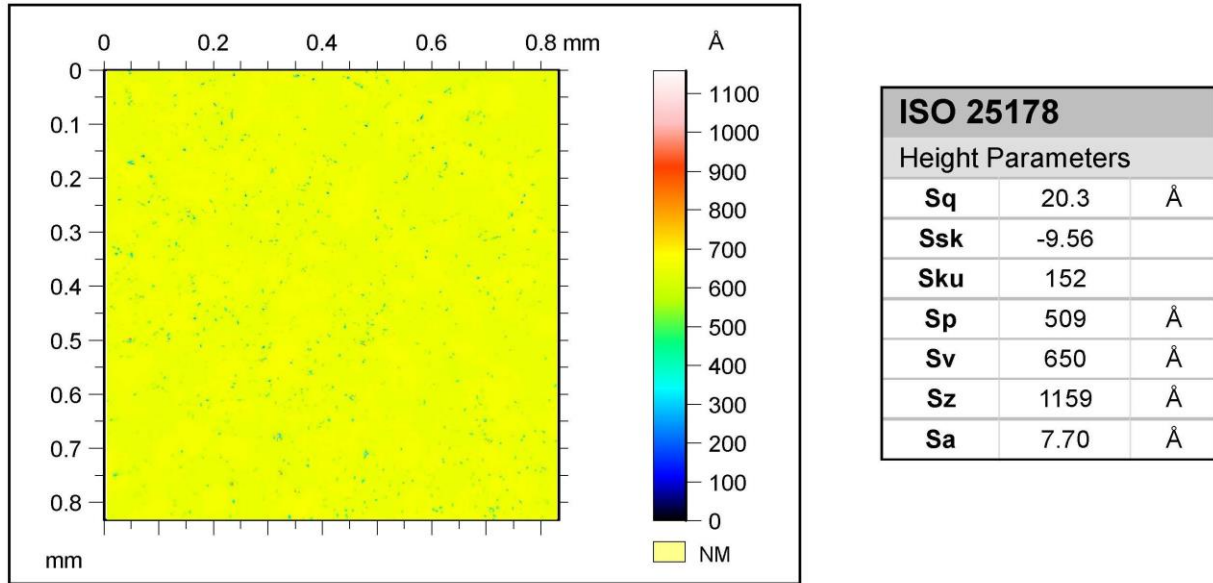


Figure 7. Surface roughness result (50 µm grain size ceramic – 20.3 Å rms (Sq))

Under the polishing conditions employed, the finer grained materials exhibited fewer and smaller pull-outs and less intergranular chipping, compared to the larger grained material. This resulted in significantly improved levels of surface roughness on the fine grained samples, with reduced polishing time required. In particular, the data show a strong trend of decreasing roughness with decreasing grain size, with the 6 µm grain size ceramic having a surface roughness below 10 Å rms. In particular, the maximum height of the peaks (Sp) drops significantly from 509 to 45 to 27 Å as the SiC particle size is reduced from 50 to 12 to 6 µm, demonstrating the enhanced polishability of the finer grain size ceramics. The trend in maximum valley depth (Sv) is not as systematic, and is believed to be due to material flaws (e.g., from subsurface damage, processing, or other) that can be addressed with further optimization. An example of a directly polished RBSC sample is provided in Figure 8.



Figure 8. Example of directly polished RBSC 100 mm diameter disc (12 µm grain size)

## 4. SUMMARY

Reaction bonded SiC ceramics were fabricated with grain sizes varying from 6 to 50  $\mu\text{m}$ , demonstrating the ability to tailor microstructure through selection of raw materials and processing parameters. The properties most affected by the change in particle size were Young's modulus, strength and thermal conductivity. As grain size increased, the SiC to Si ratio increased (i.e., better particle packing), which led to increased Young's modulus. As particle size decreased, the expected trend of increasing strength was observed due to smaller critical flaw size. Also, thermal conductivity dropped as grain size decreased due to a combination of increased interface surface area in the microstructure and lower SiC particle packing. The effect of SiC particle size (grain size) on polishability was significant. Using the same polishing parameters, the 6  $\mu\text{m}$  grain size ceramic was able to be polished to  $< 10 \text{ \AA}$  rms roughness, whereas the 50  $\mu\text{m}$  grain size ceramic could only be polished to nominally 20  $\text{\AA}$  rms roughness. These results demonstrate the ability to expand the use of RBSC ceramics to low roughness mirror applications, while eliminating the added cost and time required to apply CVD-based Si or SiC claddings. Moreover, further optimization is possible with continued optimization of the RBSC microstructure and the use of improved polishing methods for the two-phase microstructure.

## REFERENCES

- [1] Salamone, S., Karandikar, P., Marshall A., Marchant, D., and Sennett, M., "Effects of Si:SiC ratio and SiC grain size on properties of RBSC," *Ceram. Eng. Sci. Proc.* 28(2), 101-109 (2007).
- [2] Chakrabarti, O., Ghosh, S., and Mukerji, J., "Influence of grain size, free silicon content and temperature on the strength and toughness of reaction-bonded silicon carbide," *Ceramics International* 20, 283-286 (1994).
- [3] Paik, U., Park, H., Choi, S., Ha, C., and Jung, Y., "Effect of particle dispersion on microstructure and strength of reaction-bonded silicon carbide," *Mater. Sci. Eng. A334*, 267-274 (2002).
- [4] Fernandez, J., Munoz, A., Lopez, A., Feria, F., Dominguez-Rodriguez, A., and Singh, M., "Microstructure-mechanical properties correlation in siliconized silicon carbide ceramics," *Acta Mater.* 51, 3259-3275 (2003).
- [5] Aghajanian, M., Morgan, B., Singh, J., Mears, J., and Wolffe, R., "A new family of reaction bonded ceramics for armor applications," *Ceramic Transactions* 134, 527-540 (2002).
- [6] Karandikar, P., Aghajanian, M., and Morgan, B., "Complex, net-shape ceramic composite components for structural, lithography, mirror and armor applications," *Ceram. Eng. Sci. Proc.* 24(4) 561-566 (2003).
- [7] Kishner, S., Gardopee, G., Magida, M., and Paquin, R., "Large stable mirrors: a comparison of glass, beryllium and silicon carbide," *Proc. SPIE 1335, Dimensional Stability*, 127-139 (1990).
- [8] Robichaud, J., "SiC optics for EUV, UV, and visible space missions," *Proc. SPIE 4854* (2003).
- [9] Robichaud, J., Schwartz, J., Landry, D., Glenn, W., Rider, B., and Chung, M., "Recent advances in reaction bonded silicon carbide optics and optical systems," *Proc. SPIE 5868* (2005).
- [10] Schwartz, J., Arneson, A., and Robichaud, J., "Production of extreme ultraviolet (EUV) quality silicon carbide (SiC) aspheric optics," *Proc. SPIE 7018* (2008).
- [11] Duston, J., Gunda, N., Schwartz, J., and Robichaud, J., "Silicon cladding of mirror surfaces," *Proc. SPIE 7425* (2009).
- [12] Robichaud, J., Sampath, D., Wainer, C., Schwartz, J., Peton, C., and Mix, S., "Silicon carbide optics for space and ground based astronomical telescopes," *Proc. SPIE 8450* (2012).
- [13] Robichaud, J., Green, J., Catropa, D., Rider, B., and Ullathorne, C., "Silicon carbide optics for space situational awareness and responsive space needs," *Proc. Adv. Maui Optical and Space Surveillance Tech. Conf.*, E67-E71 (2008).
- [14] *Engineered Materials Handbook, Vol. 4, Ceramics and Glasses*, ASM International, Metals Park, OH, 1991.
- [15] *Metals Handbook: Desk Edition*, ASM International, Metals Park, OH, 1985.
- [16] Rice, R., Wu, C., and Borchelt, F., "Hardness-grain-size relations in ceramic," *J. Am. Ceram. Soc.* 77(10), 2539-2553 (1994).
- [17] Carroll, D., Tressler, R., Tsai, Y., and Near, C., "High temperature mechanical properties of siliconized silicon carbide composites," *Mater. Sci. Research* 20, 775-788 (1986).
- [18] Washburn, M. and Coblenz, W., "Reaction-formed ceramics," *Am. Ceram. So. Bull.* 67(2), 356-363 (1988).
- [19] Chantikul, P., Bennisson, S., and Lawn, B., "Role of grain size in the strength and R-curve properties of alumina," *J. Am. Ceram. Soc.* 73(8), 2419-2427 (1990).



- [20] Sugauma, M., Imai, T., Katayama, H., Naitoh, M., Tange, Y., Yui, Y., Maruyama, K., Kaneda, H., Nakagawa, T., and Kotani, M., "Optical testing of lightweight large all-C/SiC optics," International Conference on Space Optics, Rhodes, Greece, 2010.
- [21] Karandikar, P., Evans, G., and Aghajanian, M., "Carbon nanotube (CNT) and carbon fiber reinforced high toughness reaction bonded composites," *Ceram. Eng. Sci. Proc.* 28(6), 53-63 (2007).
- [22] Marshall, A., Chhillar, P., Karandikar, P., McCormick, A., and Aghajanian, M., "The effects of Si content and SiC polytype on the microstructure and properties of RBSC," *Ceram. Eng. Sci. Proc.* 29(2), 115-125 (2008).
- [23] Molina, J., Narciso, J., Weber, L., Mortensen, A., and Louis, E., "Thermal conductivity of Al-SiC composites with monomodal and bimodal particle size distribution," *Mater. Sci. Eng.* 480(1-2), 483-488 (2008).